I. Boxx, C. Heeger, R. Gordon, B. Böhm, M. Aigner, A. Dreizler, W. Meier, Simultaneous Three Component PIV / OH-PLIF Measurements of a Turbulent Lifted, C3H8-Argon Jet-Flame at (Sustained) 1.5 kHz Repetition Rate. Proc. Combust. Inst. 32 (1), 905-912 (2009)

The original publication is available at http://www.sciencedirect.com/

http://dx.doi.org/doi:10.1016/j.proci.2008.06.023

Simultaneous Three Component PIV / OH-PLIF Measurements of a Turbulent Lifted, C_3H_8-Argon Jet Diffusion Flame at 1.5 kHz Repetition Rate

I. Boxx[1], C. Heeger[2], R. Gordon[2], B. Böhm[2], M. Aigner[1], A. Dreizler[2], W. Meier[1]

1: Institut für Verbrennungstechnik, Deutsches Zentrum für Luft-und Raumfahrt (DLR), Pfaffenwaldring 38-40, D-70569 Stuttgart, Germany
2: Fachgebiet Energie-und Kraftwerkstechnik, Technische Universität Darmstadt, Petersenstrasse 30, D-64287 Darmstadt, Germany

Corresponding Author: Isaac Boxx, Pfaffenwaldring 38-40, D-70569 Stuttgart, Germany, Fax: (+49) 711 6862 578, e-mail: Isaac.Boxx@dlr.de

Colloquium

Diagnostics

Paper Length

- Words: 3704
- Equations: 0
- Nomenclature: 0
- Tables: 0
- References: (17+2)*7,6*2,3 = 332
- Figures and Figure Captions
  - Figure 1: (80mm + 10) * 2.2words/mm x 1 columns + (12 words) = 210
  - Figure 2: (85mm + 10) x 2.2 words/mm x 1 column + (13 words) = 222
  - Figure 3: (117.5mm + 10) * 2.2words/mm x 2 columns + (23 words) = 584
  - Figure 4: (53mm + 10) * 2.2words/mm x 2 columns + (16 words) = 293
  - Figure 5: (53mm + 10) * 2.2words/mm x 2 columns + (15 words) = 292
  - Figure 6: (75mm + 10) * 2.2words/mm x 2 columns + (24 words) = 398

Total: 3704 + 210 + 222 + 584 + 293 + 292 + 398 + 332

= 6035 words

Herewith we affirm to pay color reproduction charges for 2 figures (including both Figure 3 and Figure 4 on a single page).

Abstract

Planar Laser-Induced Fluorescence (PLIF) and stereoscopic Particle Image Velocimetry (PIV) were simultaneously applied at 1.5 kHz repetition rate to acquire time-resolved, cinematographic planar measurements of the flamebase stabilization region of a turbulent lifted jet-flame. The current work focuses on the development and demonstration of the diagnostic system and presents key examples of the new capabilities it provides. OH-PLIF is used to identify and track the spatial position and shape of the flame front near the flamebase, while the stereoscopic PIV is used to acquire three component planar velocity measurements over the same region. Initial results indicate that the significant temporal histories and experimental access to the Vz-velocity component afforded by this system are frequently essential for accurate interpretation of planar measurements in the flowfield of a lifted turbulent jet flame.

Keywords: Simultaneous kHz-PIV / PLIF; Stereoscopic; Turbulent lifted jet flame; Flame hole; Flame islands

Introduction

As demonstrated in the review papers of Pitts [1] and Lyons [2], the physical mechanism by which lifted turbulent jet flames are stabilized is an area of considerable interest to the combustion community. In particular, the degree of premixing at the flamebase and what role large-scale flow structures play in affecting this remain areas of considerable active research. Despite numerous excellent experimental, theoretical and computational studies described in these reviews, a definitive model for the physical mechanism underlying stabilization of lifted turbulent flames remains elusive.

This stems in large part from limitations associated with existing measurement techniques. Recent application of non-intrusive planar laser imaging techniques including Particle Image Velocimetry (PIV) and Planar Laser-Induced Fluorescence (PLIF) of combustion radicals to the problem have generated significant insight and yet raised interesting new questions. For example, using CH-PLIF Watson et al. [3,4] observed local discontinuities or "holes" in the flamefront of a turbulent, lifted CH_4 flame. Similar local discontinuities were observed by Hult et al. [5] in a round, unpiloted, turbulent jet flame operated close to blow-off. The existence, formation and dynamics of these holes impact our understanding of the leading edge flame structure and the degree of partial premixing at the flamebase. Subsequent experiments by Watson et al. [4,6] and Lyons et al. [7] combined sequential, two-shot CH-PLIF with 2-component PIV and showed these discontinuities to be associated with large-scale flow structures near the flamebase and interpreted them as local extinction events. Although this is undoubtedly a valid interpretation in some instances, the technique and interpretations based upon such data is inherently limited by the lack of experimental access to the Vz- (into plane, or azimuthal) velocity component. Given the highly three-dimensional nature of the lifted turbulent flamebase, this is a significant limitation. The quasi-instantaneous nature of the low repetition-rate diagnostic systems also limits one's ability to

definitively interpret even sequential two-frame (or longer) multi-shot burst planar measurements in a temporal context.

Another area of active research is that of 'flame islands' or pockets of hot, possibly reacting gases upstream and apparently distinct from the lifted flamebase. Recent computational studies by Mizobuchi et al. [8,9] suggest the presence of large diffusion flame 'islands' at the base of a turbulent jet flame. Such regions would provide heat-release and combustion radicals to significantly affect flame stabilization. The existence of such 'flame islands' was confirmed experimentally by Lyons et al. [10], who suggest they may be related to out-of-plane motion induced by filament-like secondary instabilities described in the computational study of Demare et al. [11]. The exact nature, dynamics and impact on flame stabilization of such 'islands' is still unclear. Given the unsteady nature of these islands, which appear and/or disappear within the timescale of existing imaging experiments (Lyons et al. [10]), a long-duration time-resolved planar imaging capability would be invaluable to interpreting their nature and characteristics. To quote Lyons [2], "Single shot laser imaging measurements are useful for statistical arguments, especially when acquired with other quantities such as mixture fraction, but they are not a substitute for data in time evolving format".

Recent developments in the area of high framerate CMOS imaging technology, diode-pumped solid state lasers and multistage image intensifiers have made such systems feasible. Both PIV and PLIF systems with quasi-continuous recording capabilities at multi-kHz repetition rates are beginning to come online. Wäsle et al. [12] and Kittler et al. [13] have separately (and successfully) used frequency-doubled dye lasers and intensified cameras to acquire long-duration OH-PLIF sequences in turbulent flames at kHz framerates. Upatnieks et al. [14] used a film-based PIV system to acquire 2-component velocity measurements in a lifted turbulent jet flame at 8000fps. Konle et al. [15] applied 2-component PIV and OH-PLIF simultaneously at 1-kHz to study combustion-induced vortex breakdown in a swirl burner.

Fajardo et al. [16] used a frequency-tripled solid state laser to acquire simultaneous PIV and biacetyl-PLIF measurements at 12 kHz in a non-reacting flow. Paa et al. [17] used a tuneable, frequency-tripled solid state disk laser with a 1 kHz repetition-rate to excite a hot-band transition of the OH-radical at 343nm and accomplished PLIF imaging in an industrial- and a micro-burner.

Each of these systems represents a logical and systematic extension of existing and well-developed techniques to the kHz regime, however limitations remain. To date no system has been developed to continuously track the flamefront (via a representative combustion radical) and simultaneously acquire three-component planar velocity-field measurements at high framerates and with quasi-continuous recording capability. Further development, refinement and validation of current theories on lifted flame stabilization depends upon the acquisition of time-resolved, three component velocity field data wherein the instantaneous spatial location of the flamefront is also identified and tracked. This paper describes the development and demonstration of such a system and its application to the phenomena mentioned above.

The system consists of a two-camera, stereoscopic-PIV setup and an OH-PLIF imaging system with overlapping fields of view. The system was used to acquire 3-component velocity measurements in a plane and simultaneously track the flamefront location (based on the OH-radical) at 1.5 kHz repetition rate over 1024 measurement realizations per run, or approximately 2/3 second of continuous run-time. System characteristics such as field of view, vector resolution and signal-to-noise ratio (SNR) are comparable to existing, lower framerate systems.

Experiment

The experiment configuration is illustrated in Fig. 1. The imaging region was limited to the flamebase and no attempt was made to apply this technique significantly up- or downstream of this location.

PLIF

Cinematographic OH-PLIF image sequences were acquired in the plane intersecting the jet-axis over the region of the lifted flamebase. The imaged region extended from approximately 19 to 54mm beyond the jet-exit and was positioned to the right of the jet-centerline. The cinematographic PLIF system used a frequency-doubled dye laser (Sirah, Cobra-Stretch) pumped with a frequency-doubled, diode-pumped solid state Nd:YLF laser (Edgewave IS-811E). The dye laser is modified from its original design to operate efficiently with the relatively low pulse energies produced by the pump laser at high repetition rates (7 - 12mJ, 8.5ns pulse duration). The modifications include use of only the oscillator and pre-amplifier (in a dual-level dye couvette), a high flow-rate dye circulator pump and a low-loss resonator cavity. The dye used was Rhodamine 6G and the solvent Ethanol (conc. 0.09gm/L). Under optimal operating conditions, the laser produces 0.82W (time-averaged) power at 283nm. In the present work the laser delivered 0.3W at 1.5 kHz, or 0.2mJ/pulse at 283nm. The reduced energy is believed to have resulted from a combination of sensitivity of the laser alignment and depletion of the dye solution as a result of sustained, high intensity laser-pumping. Three cylindrical lenses were used to form a sheet overlapping the imaging region. Based on a photographic paper burn pattern, the thickness of the laser sheet is estimated to have been 0.5mm in the imaging region.

Fluorescence signal was acquired with a high framerate CMOS camera (LaVision HSS5) and an external two-stage, lens-coupled intensifier (LaVision HS-IRO) with a 100mm, f/2 UV-objective (Halle Nachfl. GmbH). The camera has a 10-bit, 1k x 1k imaging array which

operates in full-frame mode up to 3000 fps and has sufficient onboard memory (2.6GB) for 2048 full-frame images. The field of view was 32mm x 32mm and overlapped that of the stereoscopic PIV cameras. Background luminosity was eliminated using a 150ns intensifier gate. Elastic scattering at 283nm was blocked using a high-transmission (> 80% at 310nm) bandpass interference filter (Custom fabrication - Laser-Components GmbH).

The low absolute pulse energy of the laser makes a shot-to-shot sheet-profile correction (e.g. by diverting a small percentage of the beam onto a fluorescing target) impossible. Therefore correction for spatial variation of the laser sheet-intensity was accomplished using a mean sheet-profile. The mean sheet-profile was determined via an ensemble average of 2048 individual images of the laser sheet passing through a dilute solution of laser dye in a target couvette placed in the center of the field of the PLIF camera. Analysis of both the individual sheet-profile images and (separately) measured pulse energies showed shot-to-shot variability to be small. As such, a mean sheet-profile correction is not expected to introduce significant error into individual images. Non-uniformity of intensifier and camera response were corrected using a 2048 shot ensemble average of a uniformly lit, white field target lamp (Kaiser Slimlite 2421).

PIV System

The stereoscopic PIV system consisted of a dual-cavity, diode-pumped, solid state Nd:YAG laser (Edgewave, ISS-411DE) and a pair of CMOS cameras (LaVision HSS5). The laser delivers 0.4mJ/pulse (or 0.65W per head at 1.5kHz), with 8.5ns pulse duration. Pulse separation for the PIV system was 50μs, with the first pulse triggered 25 μs before the OH-PLIF pulse and the second 25 μs after. Based on a photographic paper burn pattern, the sheet thickness is estimated to be approximately 0.5mm. The PIV and PLIF illumination sheets

were overlapped via a pair of dichroic mirrors. Accurate overlap was confirmed via both far-field projection and in the imaging region with a sliding knife-edge slit.

The cameras were mounted equidistance from the centerline of the PLIF camera and used 105mm, f/4 objectives (Nikon UV Micro-Nikkor) equipped with 532nm bandpass interference filters. The cameras were operated in two-frame burst mode at 1500 fps. Image-blur due to off-axis defocusing was corrected using Scheimpflug adaptors between the objectives and the cameras. Perspective distortion was corrected using a dual-plane, three dimensional imaging target (LaVision Type 7). The same target was used to map the fields of view of the stereoscopic PIV and PLIF systems to one another.

The flow was seeded with titanium dioxide (TiO_2) particles with a nominal diameter of 0.5μm via a fluidized-bed particle seeder. The jet fluid was not seeded directly as a cyclone separator unit was unavailable and experience with this system shows elastic scattering from particle agglomerations may saturate and potentially damage the intensifier. Instead, particles were seeded into the co-flow air, which has to pass through a bead bed and flow-conditioning screen prior to entering the combustion region, where they are entrained into and distributed throughout the jet fluid prior to it reaching the flamebase. This configuration resulted in relatively low seed density in the flamebase region and necessitated the delivery of additional (local) seeding to the co-flow from a secondary seeder. This was accomplished using a low-velocity, gauze-covered showerhead-type seeding nozzle placed near the outer edge of the co-flow confinement tube. The low momentum of the co-flow makes it particularly sensitive to disturbances and as such it is possible, indeed even likely that flow from the secondary seeder induced a minor asymmetric disturbance in the otherwise highly uniform co-flow. Although this possible disturbance was not rigorously characterised, we observed no alteration of gross characteristics such as liftoff height or flame stability with and without local seeding and thus

conclude that any disturbance must have been small and within the range of experimental error.

The PIV images were processed using an adaptive window offset cross-correlation algorithm implemented in a commercial analysis package (LaVision Davis 7.2). The final interrogation window was 32 × 32 pixels with a 50% window overlap, resulting in a spatial resolution of 1 mm and vector spacing of 0.5 mm. While this resolution is insufficient to resolve the smallest turbulent length-scales in the jet, it was quite sufficient for the medium and larger spatial scales around the flamebase. Although jet flows do not follow a universal scaling in the near field and we did not acquire sufficient data to rigorously determine the integral timescale for this flow, based on the downstream mean velocity profile and assuming linear growth of the jet we estimate the outer timescale of the flow to be approximately 1.3ms at the height of the flamebase. Thus, the measurement timescale (0.667ms) of our imaging system was sufficient to capture the large-scale flow structure throughout the imaging region.

Burner

The burner is shown in Fig. 1b. The fuel jet issues from a 4mm inner diameter circular tube. The tube has an external diameter of 6 mm and tapers to a sharp edge at the jet-exit. The jet tube is surrounded circumferentially to a radial distance of 63mm by a low velocity, particle-seeded co-flow of dry air. Flow-conditioning for the co-flow was accomplished via the use of a bed of glass beads, followed by a wire mesh screen.

Run Conditions

An unpiloted, circular, lifted turbulent jet diffusion-flame was studied with this system. The flame had a jet-exit Reynolds number (based on ambient temperature and pressure conditions)

of 10,000. The fuel was a 75% C_3H_8 / 25% Argon mixture and had a mean velocity of 17m/s at the jet exit. It is noted that this fuel has a significantly higher stoichiometric mixture fraction ($\xi = 0.077$) than pure propane ($\xi = 0.060$). This fuel composition offers a relatively high density and low thermal power, enabling one to achieve a turbulent lifted flame and significant lift-off height ($\approx$ 22mm, or y/d = 5.5) while maintaining a short overall flame length.

Each gas was metered separately (9.6 LPM C_3H_8, 3.2 LPM Ar) through electromechanical mass flow controllers (Brooks Model 5851) and mixed in-line over approximately ten meters of tubing prior to entering the burner. Flow-rates of the fuel and co-flow air were monitored throughout the experiment via calibration-standard Coriolis mass flowmeters (Siemens Sitrans-FC MassFlo 2100, Model DI-1.5 and DI-3). The error of these instruments at the given flowrates is specified at less than 0.3%.

Results and Discussion

Figure 2 shows a representative OH-PLIF image from the system, after sheet- and sensitivity-corrections but without smoothing or filtering. The peak PLIF signal was typically on the order of up to 128 – 130 counts, of a possible 1024. The image is indicative of the quality of the PLIF images achievable with this system.

Figure 2b shows an intensity profile taken horizontally across the image at the location shown. The profile was neither filtered, binned or otherwise smoothed and shows only minor imaging system noise. The profile also shows the gradient of the PLIF signal is noticeably higher on the inner (rich) side of the OH-zone than on the outer (lean) side. The thickness of the OH-zone varies throughout the image but is approximately 2.5mm at its widest point. The image is illustrative of the way in which the flame was consistently seen to conform to the passage of large-scale flow-structures.

Figure 3 shows a measurement sequence illustrating the advantages of long-duration temporal tracking of flow events and the importance of acquiring all three velocity components to the interpretation of experimental data in this flame. In this sequence, the corrected PLIF image is overlaid with the 3-component velocity field measurements, with vector colour representing the Vz- (through-image-plane) component of velocity. The red-green colour palette is scaled to highlight the larger magnitude (0.5 - 1.5m/s) Vz-velocities, with black representing the near-zero velocities. The absolute velocity magnitude is represented by the vector line lengths.

Figure 3 traces the appearance and development of an isolated pocket of OH upstream of the primary OH-zone. The pocket of OH is reminiscent of the flame 'islands' observed (via CH-PLIF and Rayleigh scattering) by previous researchers [10] and is likely to represent the same physical phenomenon. Frame 2 shows the appearance of this OH pocket to be associated with a region of strong, positive Vz-velocity, suggesting its sudden appearance results from out-of-plane convection of an existing flamefront. As the OH-pocket grows and deforms over Frames 3-4, the fluid in the region between the two flame fronts remains of relatively high absolute and Vz-velocity while the fluid to the lower left transitions to a negative Vz-velocity. During this interval, the two OH-zones are clearly converging upon one another, thinning somewhat as they go. In Frame 5, one sees the velocity of the fluid in the region between the two OH-zones is significantly reduced while the fluid to the left (i.e. nearer the jet-axis) remains of higher velocity. By Frame 6, the two zones have apparently merged into a single unbroken flame-front. A reasonable interpretation of this image sequence is that a region of flamefront convects into the field of view from out-of-plane, conforming to the flowfield as it goes and then merges with the existing flame associated with the primary OH-zone in the image.

Figure 3 illustrates the advantages of long-duration temporal tracking of flow-events and the importance of capturing all three components of velocity when studying a lifted flamebase. Consider, for example, Frames 4 and 5 of the sequence. If one were to acquire either measurement with a single-frame system one may easily misinterpret the data as a local extinction event, which it clearly is not. If one were to capture this event using a time-resolved planar measurement system without access to the Vz-velocity component it would be difficult to confidently interpret it as convection-related rather than perhaps auto-ignition associated with a high-temperature mixture of fuel, air and burned gas. The simultaneous time-resolved, 3-component velocity data and flame-front identification allows the quasi-convection of out-of-plane flamefront interpretation to be made with confidence and reliability.

Figure 4 shows the appearance and downstream motion of another isolated OH pocket, or flame island. As before, the appearance of the island is clearly associated with a region of strong Vz-velocity component fluid, this time in the negative (into-page) z-direction. This sequence illustrates that flame islands do not consistently occur at the outer edge of the flamebase, nor do they consistently grow in size and / or merge with the existing (outer) flamefront. A reasonable interpretation of this sequence is that a portion of the flamefront from an out-of-plane region appears in the imaging plane as a result of the strong negative Vz-velocity observable in Frame 1. It then encounters a region of high-velocity jet fluid and burns out as it is carried downstream while being starved of oxygen near the jet-core. Although the possibility of this being an auto-ignition event cannot be dismissed, the region of negative Vz-velocity associated with its appearance suggests a convection-related explanation is more likely. Such events may reasonably be expected to affect stabilization in lifted flames, providing heat-release and combustion radicals downstream of the base.

Figure 5 illustrates a possible mechanism for the apparent through-plane emergence of the flamefront. This sequence shows a moderately large flow structure impacting the base of the lifted flame. The flame distorts and then conforms to the passage of this structure, taking on a "fishhook" type configuration. In Frame 4 the end of this fishhook-shaped flame is either extinguishing or convecting out of the laser sheet. The innermost point of this fishhook structure is clearly closer to the centerline than the outermost region for any downstream location. It is straightforward to envision how such a structure would appear if viewed from an imaging plane rotated 90-degrees to the current one. It would appear as what we previously identified as a flame island, distinct from the primary flame one would expect to identify in that plane. Such fishhook shape structures are observed frequently (e.g. Fig. 2) throughout the measurement runs and may constitute the dominant mechanism responsible for the appearance of flame islands observed in lifted flames.

Figure 6 shows a flowfield event which is difficult to interpret even with the additional information afforded by this measurement system. In this sequence we see what appears to be a clear example of local extinction at a point significantly downstream of the leading edge of the flamebase. Taken in the context of the image sequence though, it is not immediately clear whether this is an extinction event in the process of occurring or the convection of a region of non-combusting fluid (possibly from a previous extinction event) through the imaging plane. The vortex (seen in Frames 2 and 3) associated with the opening of the flame discontinuity shows a strong positive Vz-velocity, suggesting a convection-induced flowfield event. The closure of this discontinuity in Frame 4 coincides with the passage of a region of strong negative Vz-velocity, suggesting it may be caused by the discontinuity convecting once more from the image plane.

It is also reasonable, however, to interpret this sequence as a local extinction event induced by shear generated by the passing vortex. Absolute strain-rates measured within and

immediately to the left of the OH-zone in Frame 2 exceed $1500s^{-1}$ and $2000\ s^{-1}$, respectively. Absolute strain rates within the flame discontinuity exceed $2000s^{-1}$ in Frame 3. The fact that the flame discontinuity collapses as the vortex passes by and the peak strain-rate within the OH region falls below $1150s^{-1}$ by Frame 5 also support the local-extinction theory. Although Lyons et al. [7] report having seen no occasions of a flamefront mending after a breach occurs the present measurements suggest this may not be uncommon.

Summary and Conclusions

A combined stereoscopic PIV / OH-PLIF system capable of quasi-continuous operation at multi-kHz framerates was developed and successfully demonstrated. Measurements were made on the base and stabilization region of a lifted, turbulent C_3H_8/Ar jet flame. Results indicate that local discontinuities observed in the flamefronts of lifted flames sometimes result from the merging and coalescence of disparate flame fronts within an imaging plane or the collapse of an existing flame hole rather than from local extinction events. Results also indicate upstream flame "islands" identified in previous research are closely coupled to out-of-plane motion of the flamefront and may be linked to the flamefront conforming asymmetrically to the passage of large-scale flow structures.

The physical interpretation of planar measurements such as these is more than an abstract or academic endeavour. Acquisition of reliable and accurate statistics and correlations relating to flowfield events depends upon the correct interpretation of information appearing in single or multi-frame planar measurements. Naturally, the greater information content of a measurement, the more reliable the interpretation may be but as Figure 6 illustrates, limitations will still exist. However, until time-resolved, simultaneous, three dimensional, three component velocity field and flame-front tracking measurement systems become

available, the system described in this work offers possibly the clearest experimental insight yet into the dynamics of a lifted turbulent flamebase.

Acknowledgements

The authors thank Chris Willert and the Institut für Antriebstechnik of DLR-Köln for the use of their fluidized bed particle seeder. The authors gratefully acknowledge the contributions of Ralf Blumenthal in preparing technical diagrams for this publication. Financial support by Deutsche Forschungsgemeinschaft through SFB 568 and GRK 1344 is kindly acknowledged.

References

[1] W.M. Pitts, Proc. Combust. Inst. 22 (1988) 809-816.

[2] K.M. Lyons, Prog. in Energy and Combust. Sci. 33 (2007) 211-231.

[3] K.A. Watson, K.M. Lyons, J.M. Donbar, C.D. Carter, Combust. Flame 117 (1999) 257-271.

[4] K.A. Watson, K.M. Lyons, C.D. Carter, J.M. Donbar, Combust. Flame 119 (1999) 199-202.

[5] J. Hult, U. Meier, W. Meier, A. Harvey, C.F. Kaminski, Proc. Combust. Inst. 30 (2005) 701-709.

[6] K.A. Watson, K.M. Lyons, C.D. Carter, J.M. Donbar, Proc. Combust. Inst. 29 (2002) 1905-1912.

[7] K.M. Lyons, K.A. Watson, C.D. Carter, J.M. Donbar, Combust. Flame 142 (2005) 308-313.

[8] Y. Mizobuchi, S. Tachibana, J. Shinio, S. Ogawa, T. Takeno, Proc. Combust. Inst. 29 (2002) 2009-2015.

[9] Y. Mizobuchi, J. Shinio, S. Ogawa, T. Takeno, Proc. Combust. Inst. 30 (2005) 611-619.

[10] K.M. Lyons, K.A. Watson, C.D. Carter, J.M. Donbar, Comb. Sci. and Tech. 179: (2007) 1029-1037.

[11] D. Demare, F. Baillot, Phys. Fluids 13(9) (2001) 2662 -2670.

[12] J. Wäsle, A. Winkler, T. Sattelmayer, Flow, Turbulence and Combustion 2005 75: 29–50.

[13] C. Kittler, A. Dreizler, Applied Phys. B, 89(2-3) (2007) 163 - 166.

[14] A. Upatnieks, J.F. Driscoll, C.C. Rasmussen, S.L. Ceccio, Combust. Flame 138 (2004) 259–272.

[15] M. Konle, F. Kiesewetter, T. Sattelmayer, Exp Fluids, (2007) Online First.

[16] C.M. Fajardo, J.D. Smith, V. Sick. Appl. Phys. B 85 (2006) 25–31.

[17] W. Paa, D. Müller, H. Stafast, W. Triebel. Appl. Phys. B 86 (2007) 1-5.

Figure Captions

Figure 1. (a) Experiment Configuration, (b) Unpiloted, non-premixed jet flame burner (c) Lifted jet flame with imaged region highlighted.

Figure 2. (A) Representative OH-PLIF Image. (B) Intensity profile over region shown.

Figure 3. OH-PLIF / PIV measurement sequence highlighting the formation, distortion and merging of a flame island. Measurement clipped to 9.5mm × 15mm.

Figure 4. Formation, convection and disappearance of a flame island. Measurement clipped to 9.5mm × 13mm.

Figure 5. Possible mechanism for upstream flame island formation. Measurement clipped to 9.5mm × 13mm

Figure 6. Appearance and disappearance of a flame-hole, possibly signifying local extinction or passage of nonburning fluid. Measurement clipped to 9.5mm × 27mm.

Figure 1.

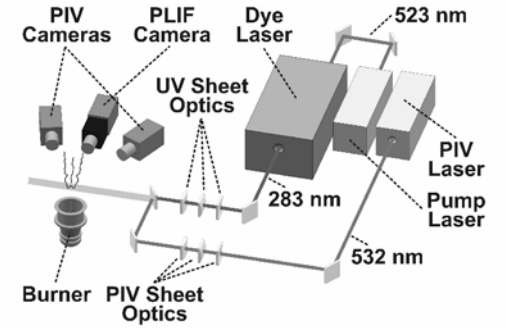
PIV
Cameras
PLIF
Camera
Dye
Laser
523 nm
UV Sheet
Optics
PIV
Laser
283 nm
Pump
Laser
532 nm
Burner
PIV Sheet
Optics

(a)

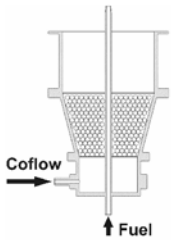
Coflow
Fuel

(b)

(c)

Figure 2.

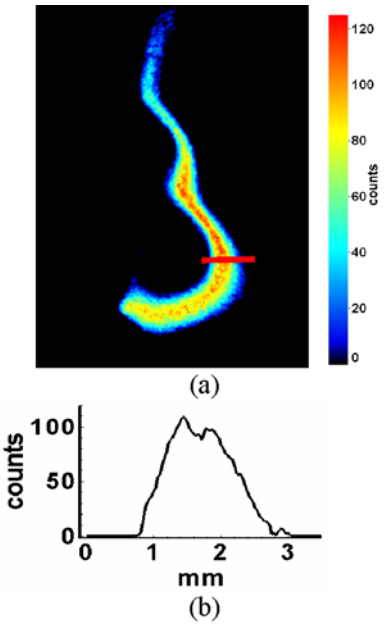

Figure 3.

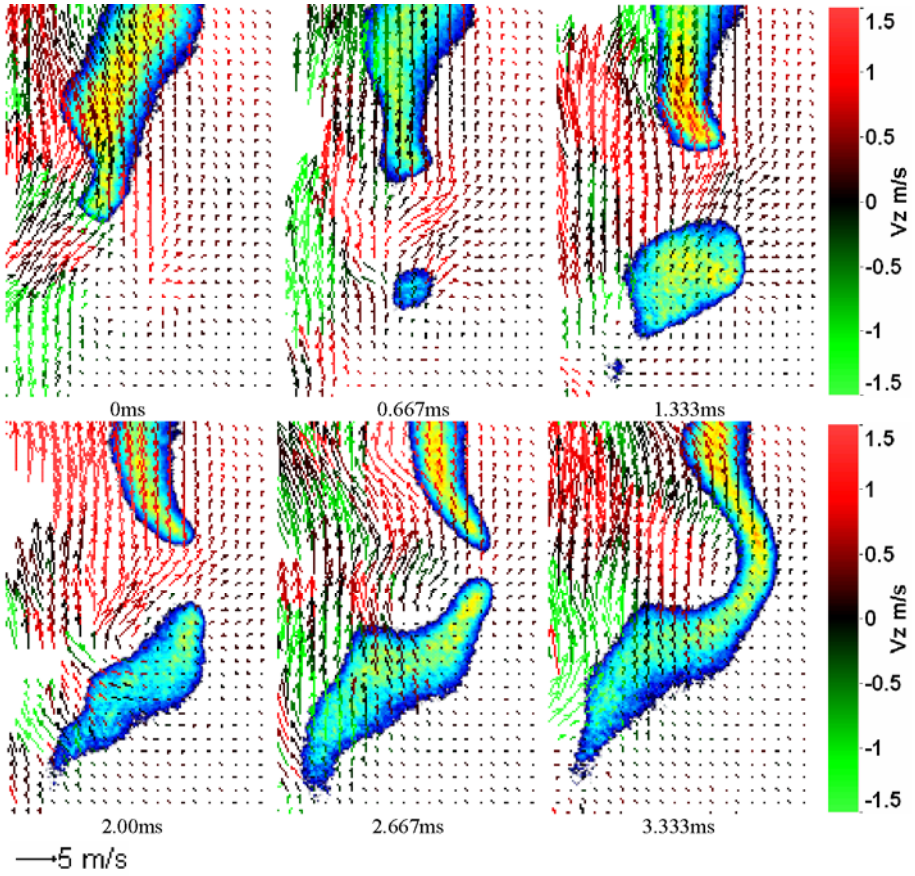
1.5
1
0.5
0
-0.5
-1
-1.5
Vz m/s
0ms
0.667ms
1.333ms
2.00ms
2.667ms
3.333ms
5 m/s

Figure 4.

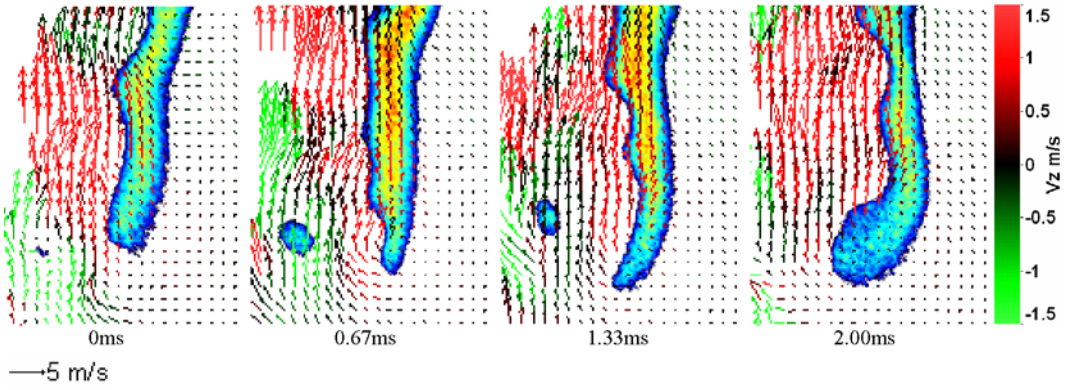

Figure 5.

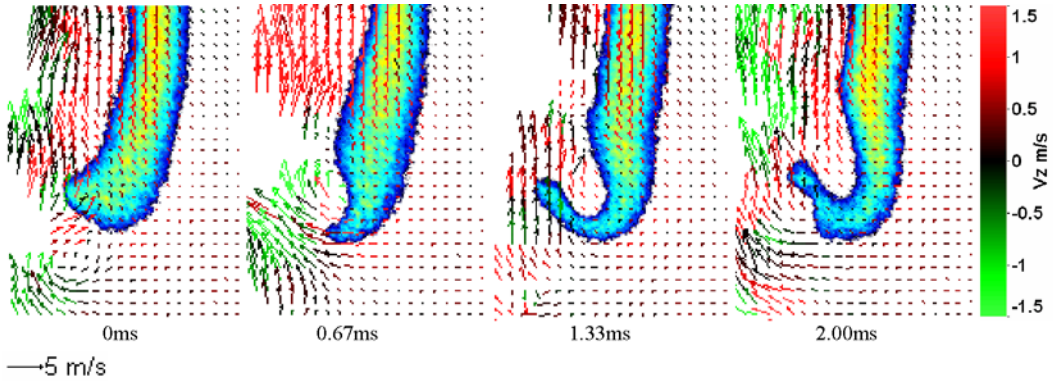

Figure 6.